IET Renewable Power Generation

Research Article

IET Journals
The Institution of Engineering and Technology

Optimal sizing method of vanadium redox flow battery to provide load frequency control in power systems with intermittent renewable generation

ISSN 1752-1416
Received on 23rd September 2016
Revised 22nd June 2017
Accepted on 7th September 2017
doi: 10.1049/iet-rpg.2016.0798
www.ietdl.org

Maximiliano Martínez[1] ✉, *Marcelo Gustavo Molina*[1], *Pedro Enrique Mercado*[1]

[1]*Instituto de Energía Eléctrica, Universidad Nacional de San Juan–CONICET, Av. Lib. San Martín Oeste 1109, J5400ARL, San Juan, Argentina*

✉ *E-mail: mmartinez@iee.unsj.edu.ar*

Abstract: This study proposes a novel methodology for optimal sizing of a vanadium redox flow battery (VRFB) aiming at providing the load frequency control (LFC) of power system (PSs) with renewable generation, such as wind generation. This methodology utilises a new optimisation problem, where the optimal size of the VRFB is an endogenous result from the model of optimisation problem. To resolve the new optimisation problem, a hybrid optimisation model (HOM) is employed in order to calculate the optimal investment for the VRFB (optimal size) while taking into account both its impact on the PS costs and on the quality of the system frequency. Through stochastic optimisation, the HOM allows computing the variable operating costs and VRFB investment costs, considering the uncertainties associated to the PS. This stochastic optimisation utilises a new quasi-stationary simulations of the PS operation, which demands lower computing effort. To this aim, this study proposes a novel modelling approach of both the VRFB and the PS operation. Moreover, statistical indexes are proposed as new factor used in sizing the LFC operating reserve. The results show that the developed methodology allows evaluating with precision the stochastic characteristics of the PS.

1 Introduction

The role of energy storage systems (ESSs) for grid applications has become more critical than ever before because of the growing penetration of intermittent renewable energy sources and the general tendency toward the deregulation and liberalisation of the wholesale electricity market. The grid integration of intermittent renewable energy sources, such as wind power generation (WPG), affects the power system (PS) operation security and the quality of the power supply due mainly to power resource instability that causes the increase of the operating reserve requirements [1, 2]. The reserve power increases the generation costs because, on one side, it imposes the need of dispatching a larger amount of generating units and, on the other side, the generating units that supply reserve must be dispatched at less efficient operating points. Moreover, a higher operating reserve decreases the probability of load disconnection. The larger the WPG penetration the higher the requirement of the operating reserve assigned to secondary frequency control, also known as load frequency control (LFC). This is because, for the 15 min–1 h time scale, load variations are more predictable than WPG variations [3].

To overcome these issues, ESSs based on advanced technologies, such as the vanadium redox flow battery (VRFB), arise as a potential alternative in order to balance any instantaneous mismatch between generation and demand in the PS by supplying LFC services. However, while ESSs offer a great flexibility, they also entail some challenges such as their installation costs due to their capital-intensive nature, which limit their application in PSs. Moreover, the reserve assigned for LFC will affect the power quality (as frequency deviations) and the operation of the PS and it is necessary to take into account these characteristics to build the optimisation model [4].

In the literature, various articles discuss both the benefits and the impact of ESSs incorporated into electrical systems with high penetration of renewable energy sources [5–9]. In [6], it is proposed a methodology to optimally determine the size of the ESS aiming at increasing the penetration level of WPG [objective function (OF)] while meeting the requirement of bounding the grid frequency deviation (restriction). This kind of research does not consider the economic impact of the ESS in the PS. In [7], the authors focus on analysing the feasibility of using large-scale energy storage to improve the predictability of wind farm production. The objective is to determine the size of a zinc–bromine flow battery and its control approach that allow reducing the energy storage investment (OF), subjected to a restriction of forecasting the power production of a wind farm. The methodology uses a dynamic simulation to evaluate the ESS operation and compares the results of different control strategies and different ESS power–energy relationships. Similarly, in [8] the authors propose a dispatch strategy which allows determining the battery capacity in a way of maximising a service lifetime/unit cost index (OF) of the ESS. This strategy is based on the statistical long-term wind speed data measured at the wind farm. In the work presented in [9], the goal is to provide tools to optimally size an ESS under the assumption that it is operated under a predictive control scheme and that the forecast of the renewable energy resources includes prediction errors. The general objective of the problem is to minimise the cost of generation of all scenarios as well as the cost of the ESS. Wind forecast errors are taken into account in the optimisation problem via probabilistic constraints for which an analytical form is derived. This allows the stochastic optimisation problem to be solved directly, without using sampling-based approaches, and sizing the storage to account not only for a wide range of potential scenarios, but also for a wide range of potential forecast errors. All the articles studied have the goal of determining the size of the ESS, which is integrated into a wind farm or is connected to the same bus of a farm, reason why it is neglected the impact of the ESS in the power flow of the electrical grid.

Other articles present algorithms to determine the optimal size of the ESSs for microgrid applications [10, 11]. For example in [10], it is proposed a robust and systematic optimal sizing algorithm for the VRFB system used in residential applications with inclusion of solar generation. The objective is to determine the optimal size of the ESS that minimises the overall electric energy cost for residential users, taking into account the battery cost and efficiency, time-varying electricity price, solar feed-in tariff, user load and photovoltaic power flow profiles. This papers models with accuracy the electrochemical characteristics of the VRFB

system, but against does not analyse the impact of the VRFB in the PS.

Additional studies present several discussions about the influence of ESSs on the electric PS reliability, as in the case presented in [12] that evaluates the impact of both wind generation and ESSs on the power grid reliability. The paper analyses different energy capacities of the ESS, several wind farm locations and various levels of restrictions in the wind generation offer. To this aim, a Monte Carlo simulation method considering the random chronological nature of the wind speed is employed and a comparison is made using a reliability index similar to the loss of load probability. In [13], a stochastic optimisation approach defines the optimal size of an ESS integrated to a thermal generation system. In this work, the OF is to maximise the incomes taking into account the life cycle cost of the ESS, production cost savings, emission savings and distribution network savings, while maintaining a specified reserve level. The decision variables are the maximum power and energy of the ESS.

Most proposals that consider the power reliability in the analysis for incorporating an ESS into the PS with inclusion of WPG do not take into account the transmission system; or, alternatively, they consider the ESS only connected to the wind farm bus. On the other hand, all these proposals discretise the computing time into 1 h intervals, which biases the ESS design towards high energy levels, and avoids evaluating the ESS influence on the LFC. Consequently, this paper has the goal of developing a methodology for optimal sizing of a VRFB that allows to calculate through probabilistic tools, generation costs, costs of energy not supplied and ESS investment costs by taking into account the ESS operation, the uncertainties associated to the stochastic nature of WPG, the availability of conventional power generation, transmission topology and power load. In addition, this model proposes to evaluate the quality of the frequency control through the efficiency factor for hourly LFC (FERSH, as Spanish acronym), as employed by the Administrative Company of the Argentinian Wholesale Electrical Market (Compañía Administradora del Mercado Mayorista Eléctrico de Argentina − CAMMESA). Eventually, in order to evaluate the benefits of this methodology, its results are compared with a technique of exhaustive search [14].

2 Optimisation problem model

The use of ESS for LFC implies an investment cost (or capital cost); therefore the ESS should be designed in such a way as to minimise the expected total cost of the PS and to maintain an adequate LFC service.

Various criteria to evaluate the performance of the LFC exist, from which it was selected the efficiency factor for hourly LFC (FERSH*)* utilised by CAMMESA. This factor is based on the concept that the LFC reaches its maximum efficiency for each hour if the slow components of the frequency are at nominal frequency at all times because, in such a case there will always be full availability of primary frequency control reserve. Appendix (Section 9.1) presents the FERSH mathematical expression. Therefore, this work proposes the index namely NCRSF (Spanish acronym) to evaluate the annual performance level of the LFC. This index is the probability that the FERSH is greater than the minimum required. This is reflected in (1) and (2), where *THs* is the sum of total hours of the simulated days

$$\mathrm{NCRSF} = 100 \times \frac{1}{\mathrm{THs}} \cdot \sum_{h=1}^{\mathrm{THs}} \mathrm{ursf}_h \tag{1}$$

$$\mathrm{ursf}_h \begin{cases} 1, & \mathrm{FERSH}_h > \mathrm{FERSH\ min} \\ 0, & \mathrm{FERSH}_h \leq \mathrm{FERSH\ min} \end{cases} \tag{2}$$

On the other hand, the problem of calculating an ESS that provides LFC to a PS is part of a planning problem for expanding the PS [15]. The solutions to this problem are tied to the PS structure which may be vertically integrated or with market-based operation. This work considers a vertically integrated structure and the static planning is carried out for a given year in the time horizon. It is also assumed that only the ESS provides LFC at all times.

Taking into account the above mentioned solution, an optimisation model is needed where $P_{\max}$ and $E_{\max}$ are an endogenous result from the model. From this condition, the OF is derived and represented in (3). It consists in minimising the expected operating costs of the PS, extended along the entire period of study, plus the annual investment costs for the ESS ($\mathrm{InvESS_{Annual}}$). The operating costs are defined as the generation costs (CostGen) plus the costs associated to energy not supplied (CostENS). In order to calculate the annual investment costs for the ESS, a precise model of the ESS that considers its service life is necessary

$$\mathrm{OF}(P_{\max}, E_{\max}) = \mathrm{ECostGen} + \mathrm{ECostENS} + \mathrm{InvESS_{Annual}} \tag{3}$$

This OF must be subject to the restriction of the performance level of the LFC. The restriction imposed onto the OF is shown in (4), where NCRSFmin is the minimum required LFC quality level

$$\mathrm{NCRSF} \geq \mathrm{NCRSF\ min} \tag{4}$$

Since the ESS performs a continuous control in which the power random variations of PS will be continuously balanced, it will be necessary to count with a chronological simulation in order to evaluate the stochastic characteristics of the PS (conventional power generation, WPG, ESS and the transmission system). This evaluation implies modelling the stochastic behaviour of the PS operation, including the random failures of system components and the stochastic fluctuations of load and WPG. Therefore, the stochastic simulation methods will be used to resolve the optimisation problem [16].

The problem of the stochastic simulation methods is the large number of PS operating simulations needed to find the expected costs and to evaluate the restrictions [16]. Therefore, this method implies enormous computing effort and computing time. However, localised high-speed computers with large-capacity storage and new techniques of parallel computing have made the stochastic simulation methods a viable option. In this work, new techniques of parallel computing will be used.

The chronological simulations can be done through the dynamic simulation of the PS. The problem that arises is the enormous computing effort and time that would be required to obtain and make a statistical evaluation of the information, so that this option cannot be applied. Therefore, this work utilises a new quasi-stationary simulation model of the PS which is solved by optimal power flows (OPF). Therefore, the new simulation methods require correct modelling of deterministic-stochastic behaviour of the system components of conventional generation, demand forecasting and wind generation. Also, the correct modelling of the corrective actions (PFC, LFC etc.) after the occurrence of the PS disturbances is necessary.

3 Power system model

3.1 Electric demand model

Electric power demand forecast is modelled through a daily load diagram partitioned into hourly schedules. The demand deviations from forecasted values to each time periods Δt are modelled through a normal distribution having a 3–7% standard deviation from the mean forecasted value [17].

3.2 Generator model

The stochastic behaviour of generators is described through the modelling of the renewable process using two states, i.e. O for ‘operating status’ and F for ‘failure status’. Therefore, the stochastic process is composed of a series of operating-failure states (Markovian process) [16].

3.3 WPG model

The WPG model is made up of a forecast model and a cost model. It is assumed that there are real data of wind power output with the necessary temporal resolution. The forecast model employed is called the persistence method [18]. The WPG deviations from forecasted values are modelled through a difference between the mean output power of the preceding hour $h-1$ (forecast for the hour h) and the real wind power outputs of each instant t at the hour h. The operating costs of wind farms are regarded negligible.

3.4 ESS model

The ESS model is developed taking into account the VRFB characteristics [19, 20], the operation mode of the ESS (it continuously balances the random variations of the PS by charging and discharging) and as it was previously mentioned the fact that in Δt time periods the ESS has already worked and the steady state is reached. Therefore, the dynamic characteristics of charge and discharge rates are not considered.

The ESS is modelled as a generator whose maximum generation limit is positive (ESS discharge) and the minimum limit is negative (ESS charge). The charge/discharge limit of an ESS is variable for each period t because it depends on the charge state of the storage device and on the maximum technical limits for charge/discharge. The maximum discharge power limit for an ESS during a period t ($\mathrm{PDESSmax}_t$) is found in (5), where $E_{t\text{-}1}$ is the available ESS energy at $t-1$, $E_{\min}$ is the minimum energy limit that the ESS can store and $P_{\max}$ is the installed discharging power of the ESS. In the same way, the maximum limit for ESS charging power at t ($\mathrm{PCESSmax}_t$) is presented in (6), where $E_{\max}$ is the maximum energy limit that the ESS can store and $P_{\min}$ is the installed charging power of the ESS

$$\mathrm{PDESS}\max_t = \min\left[\frac{(E_{t-1}-E_{\min})}{\Delta t}, P_{\max}\right] \tag{5}$$

$$\mathrm{PCESS}\max_t = \max\left[\frac{(E_{t-1}-E_{\max})}{\Delta t}, P_{\min}\right] \tag{6}$$

The energy in the ESS at the end of any t (E_t) is dependent on $E_{t\text{-}1}$, the charging or discharging during a Δt time lapse before t and on the ESS efficiency at t (η_t). This is expressed in (7) and (8), where PESS_t is the charge or discharge power at time t. On the other hand, η_{charge} and $\eta_{\mathrm{discharge}}$ are the charge and discharge efficiencies of the ESS, respectively [21]

$$E_t = E_{t-1} - \eta_t \cdot \mathrm{PESS}_t \cdot \Delta t \tag{7}$$

$$\eta_t \begin{cases} \eta_{\mathrm{charge}}, & \mathrm{PESS}_t < 0 \\ \eta_{\mathrm{discharge}}, & \mathrm{PESS}_t > 0 \end{cases} \tag{8}$$

The model for investment costs in US$/h is stated in (9), where H is the mean service life of an ESS, and c_{P}, $c_{\mathrm{E}}$are the costs per installed power and energy unit of the ESS. Since the service life of the ESS is expressed as charge–discharge cycles, it is necessary to change this unit to years, using the expression (10). There, LS is the lifespan of the ESS stated as charge–discharge cycles; C.Annual is the average annual charge–discharge cycles of the ESS. The determination of C.Annual is dependent on the ESS control strategy, and it is calculated from the results of the chronological simulations [21]

$$\mathrm{InvESS}_{\mathrm{Annual}} = \frac{(c_{\mathrm{P}} \cdot P_{\max} + c_{\mathrm{E}} E_{\max})}{(8760 * H)} \tag{9}$$

$$H = \frac{\mathrm{LS}}{\mathrm{C.Annual}} \tag{10}$$

4 Power system operation model

In this work, a novel quasi-stationary simulation model has been adopted. These timed simulations discretise the analysis time into short time periods (Δt) where stationary conditions for the PS are considered. PS operation is represented by a dispatch/re-dispatch model that simulates the operator actions and another operation model between dispatches that emulates the automatic corrective actions (PFC, LFC etc.).

4.1 Emulation of the daily operation program and operator corrective actions

The hourly dispatch and the operator corrective actions (non-automatic corrections) are modelled as the result from OPFs that comply with the demand forecast for each hour (h), considering the WPG forecast and the available units at each hour. This optimisation is performed by satisfying the distribution of PFC reserve and minimised the generation costs (includes WPG costs).

4.2 Emulation of automatic corrective actions

The difference between the generation determined by the above model and the demand resulting from disturbances is compensated by the automatic corrective actions of the PS. The unbalances are corrected basically by the activation of the PFC, the LFC available in the ESS, the decrease of WPG and the disconnection of loads.

This work considers to discretise the load diagram in a few minutes and it is considered that in these periods, the steady state is reached after the perturbation. In these periods, it is considered that the PFC acts first and then the LFC. Therefore, the LFC reserve replaces the PFC reserve, so that only the action of LFC reserve is observed at the end of the period. If the LFC reserve is not enough, both reserves will compensate the unbalances at the end of the period t, leaving a frequency deviation of the nominal value. This frequency deviation depends of PFC power supplied at the end of the period t and of speed-droop characteristic of the PS. If the LFC and PFC reserves are not enough, both reserves and load disconnection compensate the unbalance at the end of the period t. Consequently, the emulation of automatic corrective actions must follow the following sequence: first the action of the ESS (supplier LFC), then the reserve of PFC and finally the load disconnection. In case of excess generation, WPG is decreased after the action of the ESS and the PFC reserve.

The mathematical model is formulated as an OPF problem with additional generating units that are fictitious in the PS but represent the automatic corrective actions mentioned above. These non-existent units are necessary for the new quasi-stationary modelling stated here and are called ‘virtual units’. The virtual units represent the ESS charge/discharge (ESS virtual unit), the increase or decrease of the output power of units that supply PFC (PFC virtual units) and the disconnected load (virtual disconnected load unit). For example, in Fig. 1 it is shown how the virtual unit of the PFC (G*v* PFC) is used to simulate the operation of a conventional generator (G1) which provides PFC. Power generator scheduled for G1 in the interval h is represented by the generator ‘G*n* Dis’ and the PFC of generator G1 is represented by the virtual unit ‘G*v* PFC’. Therefore, the output power of generator G1 for each instant t is represented by the sum of G*v* PFC output power and G*n* Dis output power.

Optimisation of virtual units is performed by satisfying an OF for minimising their generation costs. Consequently, this optimisation uses the costs and technical restrictions of the virtual units in a way as to represent correctly, and in a proper sequence, the performance of the corrective actions. Fig. 2 shows the cost functions for virtual units.

The variations in output power of units that supply PFC ($\Delta PG_{i,t}$) at instant t (where stationary conditions are reached) is proportional to the governor speed-droop characteristic of each unit (R_i) and the system frequency deviation (Δf_t) at such instant t [4]. This relationship can be seen in the following equation:

$$\Delta PG_{i,t} = -\frac{\Delta f_t}{R_i} \tag{11}$$

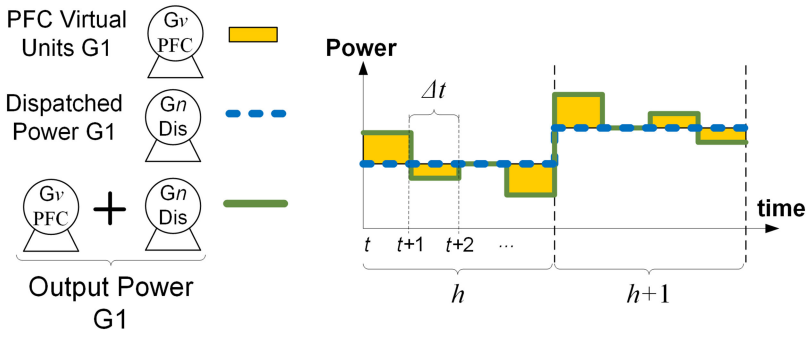

Fig. 1 *Representation of generator using virtual units*

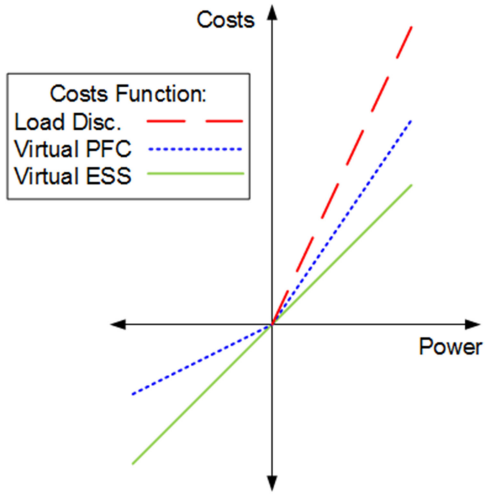

Fig. 2 *Linear cost functions for virtual units*

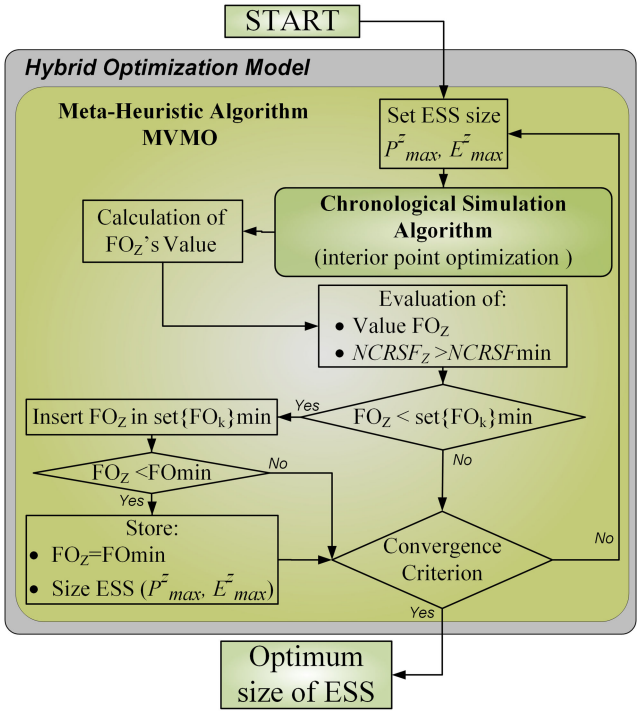

Fig. 3 *Proposed HOM*

Therefore, the composite power/frequency characteristic of a PS depends on the combined effect of the droops of all generator speed governors [4]. Hence, if there are variations in output power of units that supply PFC ($\Delta PG_{i,t}$), there is a frequency deviation. Considering that power variations will be represented by the output power of the virtual units PFC ($PGv_{i,t}$), then the system frequency deviation Δf_t can be computed by expression (12) where Ng is the number of units supplying primary frequency control at instant t. The next step is to calculate FERSH of each hour of simulation and with these values compute the value of NCRSF.

$$\Delta f_t = -\frac{\sum_{i=1}^{Ng}\Delta PG_{i,t}}{\sum_{i=1}^{Ng}(1/R_i)} = -\frac{\left(\sum_{i=1}^{Ng}\Delta PG_{i,t}\right)\cdot\prod_{i=1}^{Ng}R_i}{\sum_{i=1}^{Ng}R_i} = -\frac{\left(\sum_{i=1}^{Ng}PGv_{i,t}\right)\cdot\prod_{i=1}^{Ng}R_i}{\sum_{i=1}^{Ng}R_i} \quad (12)$$

5 Hybrid optimisation model (HOM)

A HOM is proposed in this work to find the optimal size of the ESS. This HOM uses a primal–dual interior point algorithm [22] embedded in a meta-heuristic algorithm. The ESS size optimisation is carried out using the *meta-heuristic algorithm* and the primal–dual interior point algorithm is used inside *chronological simulations algorithm* to solve OPFs. Any of the various meta-heuristic methodologies available to date can be applied to solve this optimisation problem, although with dissimilar efficiencies, according to the 'no free lunch' theorem. It is so, since the proposed optimisation problem has different characteristics compared with the optimisation problems of reserve and planning commonly used in the PS [23]. So, it is proposed to use a meta-heuristic algorithm called mean variance mapping optimisation (MVMO) for the optimisation of the ESS size [24].

Fig. 3 shows the proposed HOM. The algorithm begins with the *meta-heuristic algorithm* MVMO that uses $P_{\max}$ and $E_{\max}$ as decision variables. The optimisation processes choose any given size of the ESS $\left(P^Z_{\max}, E^Z_{\max}\right)$ through a uniform distribution; then it sends these data to the *chronological simulation algorithm* aiming at performing *Nd* simulation days of the PS operation with the selected ESS size to obtain the statistical variables for calculating the OF and its restrictions. The *Nd* simulations must be such as to ensure the statistical convergence of the OF [25]. The results are evaluated and if the solution meets the restriction and the value of the OF are less than some value of all the best solutions so far (set {OF}min), the algorithm stores this value in the set of best solutions [24]. If the new solution has a FO_Z value less than the best solution ($FO_{\min}$), it becomes the best solution until now and is used for the analysis of convergence of meta-heuristic algorithm. If the convergence criterion is not reached, the algorithm changes the ESS size in the block *Set ESS size* [24]. From here, the process is repeated until the optimum size of the ESS is obtained.

The flowchart of *chronological simulation algorithm* can be seen in Fig. 4. The algorithm begins with the reading information from the PS data and the ESS size $\left(P^Z_{\max}, E^Z_{\max}\right)$. Then, the algorithm calculates the demand and availability of the generating units. After that, it is calculated the WPG forecast and the generating units availability for each h interval. With this information, the block *emulation of operator actions* calculates the generating units' initial output power for the interval h through OPFs. Subsequently, automatic corrective actions of the PS are simulated, inside the block *emulation of automatic actions*, with basis on the initial output powers of the units. Once the emulation of automatic actions is made for the h interval, it proceeds to store data of

power, frequency deviations and total power generated by each unit in each interval of time t within the hour h. Subsequently, the algorithm continues with the next hour h until completing the review of all hours of the day analysed (Hd). Then, it proceeds to calculate the FERSHs, the generation costs and the ENS of the examined period. After that, the algorithm continues with the next nd day and this process is repeated Nd times. With data accumulated, they are calculated the expected generation costs, the expected ENS costs, the NCRSF and the average annual cycles of charge–discharge reached by the ESS size selected. These variables are the output of the algorithm.

6 Simulation results: calculation of the optimal size of a VRFB

For the purpose of this work, a small PS has been modelled, as depicted in Fig. 5. The Appendix (Section 9.2) presents the characteristics of the VRFB, the PS and the WPG used. It is assumed that NCRSFmin is 99% and 730 simulations of 24 h with a time resolution of 5 min (Δt) are used to ensure statistical convergence of total costs.

Table 1 shows the MVMO parameterisation. The decision variables ranges are from 0 to 50 MW and 0 to 50 MWh, and the MVMO begins in the mean value of the range of each decision variable.

The models, algorithms and simulations have been performed with MATPOWER 6.0b [26] running on the MATLAB/Simulink environment and the generator block time-based pseudorandom number was used. The calculation is distributed in a cluster of 24 computers with Intel i7-2600K 4 cores with 8 threads and a speed of 3.4 GHz.

Table 2 shows the results obtained by applying the HOM. There, it can be noted that the optimal VRFB size is 9 MW and 10 MWh; the NCRSF achieved is 99.1% just above the NCRSFmin and the total costs per hour reached is 2214 US$/h. The total costs are composed of the expected generation costs (about 91%) predominantly, then the annualised investment cost (about 7%) and lastly the expected ENS costs (about 2%). The investment cost on this VRFB ESS is US$ 23.5m and the mean service life achieved is 17.4 years.

To evaluate the benefits of the HOM and if this algorithm reached the optimum, an exhaustive search of power and energy VRFB values is performed and the results are compared with the results of the HOM. The exhaustive search method is a general technique for solving optimisation problems, where a thorough and systematic search is done throughout the solution space to find the optimal solution. This technique ensures to find the global optimum of the optimisation problem. The results achieved are presented in Table 2.

The optimal VRFB size obtained by exhaustive search is consistent with that obtained by the HOM, with the difference in the calculation time. To verify the robustness of the HOM, 20 optimisations of the VRFB size were performed, achieving a 95% success in optimisations. This shows the great effectiveness of the proposed algorithm to find the optimal solution. The difference between the proposed algorithm and exhaustive search method is in efficiency of both methods, the HOM needs 17.33% (13 h) of the time required by the exhaustive search (75 h) and this is extremely important to resolve larger PSs.

Fig. 6 shows the evolution of total costs for the range from 0 to 25 MW and 0 to 25 MWh.

It shows that the minimum value of the total cost is obtained for 4 MW and 4 MWh values, but this relationship does not meet the restriction of NCRSFmin (99%). The figure shows the combination of power and energy values that meet the restriction (suitable NCRSF zone) and the minimum value of the total cost for this zone (9 MW and 10 MWh), equal to the results obtained with the proposed HOM. Fig. 6 shows the complexity of the total cost function and that the restriction of NCRSFmin is important to determine the optimal VRFB size.

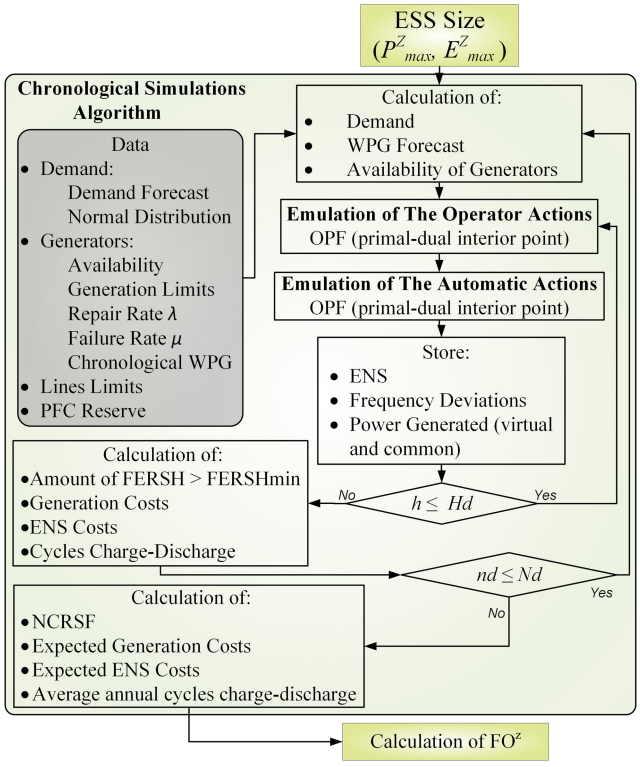

Fig. 4 *Chronological simulation algorithm*

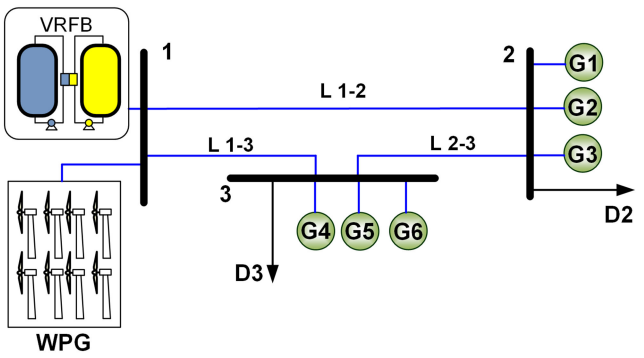

Fig. 5 *System model of three nodes*

Table 1 MVMO parameters

Max iter.	No. of iter. without improvement	Selection method	No. of best solution	Mutation variables	Initial scale factor	Final scale factor	Initial d factor	Δd
500	50	2	4	1	1	1	1	0,25

Table 2 VRFB optimisation results

Method	Optimal P_{max}, MW	Optimal E_{max}, MWh	NCRSF, %	Exp. gen. costs, US$/h	Exp. ENS costs, US$/h	Ann. inv. cost, US$/h	Total cost, US $/h	Time, h
HOM	9	10	99.1	2006	54	154	2214	13
exhaustive	9	10	99.1	2006	54	154	2214	75

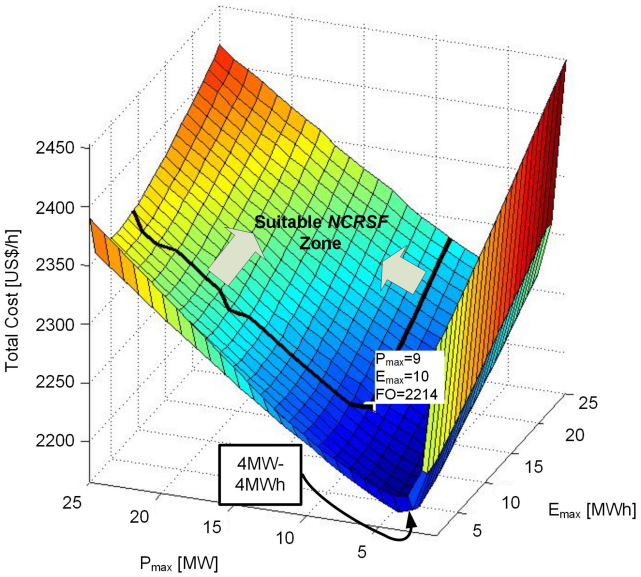

Fig. 6 *Evolution of total costs and NCRSF limits for the range from 0 to 25 MW and 0 to 25 MWh*

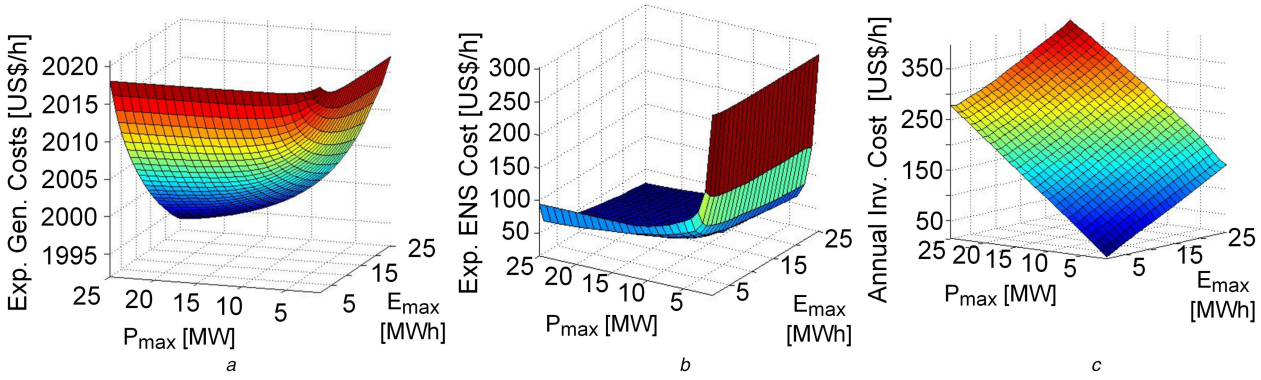

Fig. 7 *Evolution of total costs components*
(a) Expected generation costs, ***(b)*** Expected ENS costs, ***(c)*** Annualised investment costs

The evolution of the expected generation costs, the expected ENS costs and annualised investment cost as function of the VRFB power and energy is shown in Figs. 7*a–c*, respectively. As shown in Fig. 7*a*, the expected generation costs decrease as VRFB capacities grow in both power and energy. This is because the increase of VRFB size reduces the activation time of PFC and therefore the generation cost is reduced. Furthermore, as shown in Fig. 7*b*, the expected ENS costs decrease as VRFB capacities grow in both power and energy, although this effect is more sensitive to increased power capacity that to increase the energy capacity. This is because the increase of VRFB size, especially in power capacity, reduces the outage time and therefore the expected ENS costs. On the other hand, the annualised investment costs (Fig. 7*c*) increase, practically linearly as VRFB capacities grow in both power and energy. This is because the average annual charge–discharge cycles of VRFB practically do not change with power and energy capacity. Therefore, the mean service life in years practically does not change too and for this reason, according to (10), the annual investment costs vary practically linearly with power and energy capacities.

While the expected generation costs are the largest component of total costs, they do not present major changes. The maximum difference of the expected generation costs for the exploration area (the difference between its maximum and minimum) is 25.94 US $/h. On the other hand, the expected ENS costs and annualised investment costs vary greatly throughout the explored area. The maximum difference of the expected ENS cost is 262.22 US$/h and for the annual investment cost is 377.72 US$/h. Therefore, for this PS, the VRFB optimal size is a trade-off between the annualised investment costs and the expected costs of ENS.

7 Conclusion

This paper has presented a novel methodology for optimal sizing, and therefore optimal investment, of a FRFB. This methodology employs a new optimisation problem that is solved via a HOM. By using a new quasi-stationary simulations of the PS operation with reduced computing effort, the proposed HOM allows computing all the variables required by that optimisation. For these simulations, this work proposes a novel model of a VRFB and PS operation. In order to analyse the influence of the VRFB on the PS frequency quality, statistical index was proposed as a new factor (index for LFC quality level) used in sizing the LFC operating reserve. The results show the great effectiveness of the proposed methodology to model the PS operation and find the optimal solution. On the other hand, the HOM proved to have a good efficiency in the time required to solve the optimisation problem, which permits to extend the proposed algorithm to solve larger PSs. In addition, the results show the influence of NCRSF in determining the optimal size of the VRFB. This is the case because without this, the VRFB may be undersized and then reach less total costs but not meeting the LFC quality standards required by the PS.

On the other hand, the annualised investment cost depends on the service life cycles of the VRFB and on their average annual charge–discharge cycles. The annual average cycles and the NCRSF depend on the network topology, the stochastic nature of their components and the VRFB size. Therefore, these variables can be determined only from the stochastic time simulations applied through the proposed calculation model.

The novel methodology presented in this work allows evaluating with precision the stochastic characteristics of the overall operation of the conventional generation, WPG, transmission system, VRFBs and the corrective actions. This

evaluation also allows observing how this overall operation affects the generation costs, costs of ENS, investment costs and the system frequency quality.

8 Acknowledgements

This work has been supported by ELAC2014/ESE0034 from the European Union and its linked Argentinean national project 018/16, Res. MINCYT 542/15. We also appreciate the support from Argentinean National Agency for the Promotion of Science and Technology (ANPCyT) through projects PICT-2012-1733 and PICT-2015-2963, the National Council for Science and Technology Research (CONICET), and the National University of San Juan (UNSJ).

9 References

[1] European Commission: http://ec.europa.eu/energy/renewables/, accessed 27 December 2015
[2] 'U.S. Department of Energy, Database of State Incentives for Renewables & Efficiency'. Available at http://www.dsireusa.org/summarymaps/, accessed 20 July 2015
[3] Ackermann, T.: '*Wind power in power systems*' (John Wiley & Sons, 2005, 2012, 2nd edn.)
[4] Kundur, P.: '*Power system stability and control*' (McGraw-Hill, 2001)
[5] Niu, Y., Santoso, S.: 'Sizing and coordinating fast- and slow-response energy storage systems to mitigate hourly wind power variations', *IEEE Trans. Smart Grid*, 2016, **PP**, (99), pp. 1–1
[6] Liu, Y., Du, W., Xiao, L., *et al.*: 'A method for sizing energy storage system to increase wind penetration as limited by grid frequency deviation', *IEEE Trans. Power Syst.*, 2016, **31**, (1), pp. 729–737
[7] Brekken, T., Yokochi, A., Von Jouanne, A., *et al.*: 'Optimal energy storage sizing and control for wind power applications', *IEEE Trans. Sustain. Energy*, 2011, **2**, pp. 69–77
[8] Li, Q., Choi, S.S., Yuan, Y., *et al.*: 'On the determination of battery energy storage capacity and short-term power dispatch of a wind farm', *IEEE Trans. Sustain. Energy*, 2011, **2**, (2), pp. 148–158
[9] Baker, K., Hug, G., Li, X.: 'Energy storage sizing taking into account forecast uncertainties and receding horizon operation', *IEEE Trans. Sustain. Energy*, 2017, **8**, (1), pp. 331–340
[10] Zhang, X., Li, Y., Skyllas-Kazacos, M., *et al.*: 'Optimal sizing of vanadium redox flow battery systems for residential applications based on battery electrochemical characteristics', *Energies*, 2016, **9**, (10), p. 857
[11] Chen, S.X., Gooi, H.B., Wang, M.Q.: 'Sizing of energy storage for microgrids', *IEEE Trans. Smart Grid*, 2012, **3**, (1), pp. 142–151
[12] Hu, P., Karki, R., Billinton, R.: 'Reliability evaluation of generating systems containing wind power and energy storage', *IET Gener. Transm. Distrib.*, 2009, **3**, pp. 783–791
[13] Chakraborty, S., Senjyu, T., Toyama, H., *et al.*: 'Determination methodology for optimising the energy storage size for power system', *Gener. Transm. Distrib.*, 2009, **3**, (11), pp. 987–999
[14] Wang, X., Zhang, X., Dong, L., *et al.*: 'Development of methods for beam angle optimization for IMRT using an accelerated exhaustive search strategy', *Int. J. Radiat. Oncol. Biol. Phys.*, 2004, **1**, pp. 1325–1337
[15] Pringles, R.M., Olsina, F., Garcés, F.: 'Designing regulatory frameworks for merchant transmission investments by real options analysis', *Energy Policy*, 2014, **67**, pp. 272–280
[16] Billinton, R., Li, W.: '*Reliability assessment of electric power systems using Monte Carlo methods*' (Plenum, New York, 1994)
[17] Hong, T., Gui, M., Baran, M.E., *et al.*: 'Modeling and forecasting hourly electric load by multiple linear regression with interactions'. IEEE Power and Energy Society General Meeting, 2010, 2010, pp. 1–8
[18] 'Bonneville Power Administration. How BPA supports wind power in the Pacific Northwest'. Available at http://www.bpa.gov/corporate/pubs/fact_sheets/09fs/BPA_supports_wind_power_for_the_Pacific_Northwest_-_Mar_2009.pdf, accessed 3 December 2013
[19] Molina, M.G.: '*Emerging advanced energy storage systems: dynamic modeling, control and simulation*' (Nova Science Pub. Inc., New York, 2013, 1st edn.)
[20] Ontiveros, L.J., Mercado, P.E.: 'Thyristor-based flexible ac transmission system for controlling the vanadium redox flow battery', *IET Renew. Power Gener.*, 2013, **7**, (3), pp. 201–209
[21] Chen, H., Cong, T.N., Yang, W., *et al.*: 'Progress in electrical energy storage system: a critical review', *Prog. Nat. Sci.*, 2009, **19**, (3), pp. 291–312
[22] Lustig, J., Marsten, R.E., Shannon, D.F.: 'Computational experience with a primal–dual interior point method for linear programming', *Linear Algebr. Appl.*, 1991, **2**, (4), pp. 575–601
[23] Wolpert, D.H., Macready, W.G.: 'No free lunch theorems for optimization', *IEEE Trans. Evolut. Comput.*, 1997, **1**, (1), pp. 67–82
[24] Erlich, I., Venayagamoorthy, G.K., Worawat, N.: 'A mean-variance optimization algorithm'. Proc. WCCI 2010 IEEE World Congr. Computational Intelligence (CCIB), Barcelona, Spain, July 18–23, 2010
[25] Sumathi, S., Hamsapriya, T., Surekha, P.: '*Evolutionary intelligence: an introduction to theory and applications with Matlab*' (Springer, 2008)
[26] Zimmerman, R.D., Murillo-Sánchez, C.E., Thomas, R.J.: 'MATPOWER: steady-state operations, planning and analysis tools for power systems research and education', *IEEE Trans. Power Syst.*, 2011, **26**, (1), pp. 12–19
[27] CAMMESA: 'Procedimientos para la Programación de la Operación, el Despacho de Cargas y el Cálculo de Precios', Nov 1998, Anexo 23: Regulación de frecuencia, Procedimiento técnico N° 9: Participación de los generadores en el servicio de regulación de frecuencia del MEM (in Spanish)
[28] 'Wind Energy in Australia: Wind Farm Performance'. Available at http://windfarmperformance.info/, accessed 9 July 2014

9 Appendix

9.1 FERSH mathematical expression

Given the droop characteristics of a PS and its PFC reserve level, there exists a disturbance that causes a frequency deviation that depletes the reserve assigned to PFC (Δfmx). Upon defining Δfmx, it is then proceeded to establish the FERSH for each hour period according to (13), where ΔfFP_h is the mean value of filtered frequency deviations at hour h [27]

$$\mathrm{FERSH}_h = 1 - |\Delta fFP_h / \Delta fmx| \tag{13}$$

For simplicity, in order to calculate ΔfFP_h for each hour of the period analysed, this work considers that each hour h of simulation is discretised in short time periods (Δt) of few minutes (5 min). In this short time periods it is considered that the LFC already worked and the steady state is reached. In this way, for each Δt, it can be calculated a frequency deviation. Therefore, for simplicity, ΔfFP_h will be calculated as the mean value of frequency deviations at hour h. In addition, in order to regard the LFC acceptable, the value of FERSH_h must be greater than a minimum (FERSHmin) set by the system operator [27].

9.2 Characteristics of the VRFB, the PS and the WPG

Table 3 shows the characteristic of VRFB [19]. Table 4 presents the characteristics of the generating units (maximum and minimum capacities, droop characteristics, coefficients of polynomials costs, failure rates λ and repair rates μ) [12]. The power lines share the same characteristics, with 0.13 p.u. inductive reactance and 60 MW power capacity. The simulation time is discretised into 5 min intervals. The system frequency excursion is limited to ± 800 mHz. On the other hand, the amount for value of lost load (VOLL) is assumed as 1000 US$/MWh. The operating reserve assigned to PFC is 15% of the power load.

For the case of the WPG, the data were obtained from the Woolnorth-Australia wind farm having 140 MW of installed power [28]. For calculations, two scenarios have been considered, i.e. scenario 1 considers the output power data for year 2010, whereas scenario 2 those data for year 2012 [28]. Table 5 shows the characteristics of demand for both scenarios as a percentage of maximum demand (314 MW). Table 6 shows the availability and power reserve provided by the generating units for both scenarios.

Table 3 VRB characteristics

Characteristic	Unit	VRB
available power range	MW	0.01-50
available energy range	MWh	0.01-50
charge–discharge efficiency	%	90-85
lifespan	cycles	12,000
power investment cost	US$/kW	1500
energy investment cost	US$/kWh	1000

Table 4 Characteristics of the generating units

Gen.	Power		C_0	C_1	R	λ	μ
	Min	Max					
	MW	MW	US$/h	US$/MWh	%	1/h	1/h
WPG	0	140	0	0	—	—	—
G1	23	76	87	15	6	1/1960	1/40
G2	8	25	9	104	4	1/450	1/50
G3	30	100	34	105	4	1/450	1/50
G4	47	155	124	12	5	1/960	1/40
G5	15	50	14	1	4	1/1980	1/20
G6	30	100	34	105	4	1/450	1/50

Table 5 Power demand data

Hour	Sce.1		Sce.2		Hour	Sce.1		Sce.2	
	N2	N3	N2	N3		N2	N3	N2	N3
	%	%	%	%		%	%	%	%
6:00	25	36	26	38	18:00	33	49	34	44
7:00	25	37	27	39	19:00	37	55	39	49
8:00	27	39	29	39	20:00	40	60	42	56
9:00	28	41	30	41	21:00	37	56	40	60
10:00	29	43	31	44	22:00	28	42	30	51
11:00	31	45	33	47	23:00	23	34	24	45
12:00	30	44	32	50	00:00	21	31	22	36
13:00	29	42	31	46	1:00	19	28	20	33
14:00	27	40	29	45	2:00	18	27	19	30
15:00	25	37	27	41	3:00	19	28	20	29
16:00	27	39	28	37	4:00	21	31	22	30
17:00	29	43	31	41	5:00	24	36	25	33

Table 6 Availability of units and power reserve type

Period	Gen.	Sce. 1		Sce. 2	
		Type reserve	State	Type reserve	State
18 to 22 h	G1	PFC	rotating	PFC	rotating
	G2	PFC	rotating	PFC	rotating
	G3	tertiary	stop	tertiary	stop
	G4	PFC	rotating	PFC	rotating
	G5	PFC	rotating	—	—
	G6	tertiary	stop	tertiary	stop
6 to 17 h	G1	PFC	rotating	PFC	rotating
	G3	tertiary	stop	tertiary	stop
	G4	PFC	rotating	PFC	rotating
	G5	PFC	rotating	—	—
	G6	tertiary	stop	tertiary	stop
23 to 5 h	G3	tertiary	stop	tertiary	stop
	G4	PFC	rotating	PFC	rotating
	G5	PFC	rotating	—	—
	G6	tertiary	stop	tertiary	stop